



The role of laboratory testing in the development of rotor aerodynamics (review)

Okulov, Valery

Published in:
Thermophysics and Aeromechanics

Link to article, DOI:
[10.1134/S0869864318010018](https://doi.org/10.1134/S0869864318010018)

Publication date:
2018

Document Version
Peer reviewed version

[Link back to DTU Orbit](#)

Citation (APA):
Okulov, V. (2018). The role of laboratory testing in the development of rotor aerodynamics (review). *Thermophysics and Aeromechanics*, 25(1). <https://doi.org/10.1134/S0869864318010018>

General rights

Copyright and moral rights for the publications made accessible in the public portal are retained by the authors and/or other copyright owners and it is a condition of accessing publications that users recognise and abide by the legal requirements associated with these rights.

- Users may download and print one copy of any publication from the public portal for the purpose of private study or research.
- You may not further distribute the material or use it for any profit-making activity or commercial gain
- You may freely distribute the URL identifying the publication in the public portal

If you believe that this document breaches copyright please contact us providing details, and we will remove access to the work immediately and investigate your claim.

1

2

DOI: 10.1134/S0869864318010018

3

The role of laboratory testing in the development of rotor aerodynamics (review)*

4

5

V.L. Okulov

6

The Technical University of Denmark, Lyngby, Denmark

7

Kutateladze Institute of Thermophysics SB RAS, Novosibirsk, Russia

8

E-mail: vaok@dtu.dk

9

(Received July 5, 2017; in revised form September 7, 2017)

10

11

12

The aim of the review is to assess the value of model experimental studies for the development of classical rotor aerodynamics as well as to describe the most significant recent results stimulated by intense development of wind power.

13

14

Key words: rotor aerodynamics, vortex wake behind the rotor, wind power plant, interaction between the rotor and the wake, power loss.

15

Introduction

16

17

18

19

The current stage of rotor aerodynamics development is undoubtedly associated with the development of wind power, with the transition from single wind turbines to a network of wind power plants (WPP) and their transformation into the industrial sector — the most important component of the global energy potential (Gupta, 2015).

20

21

22

23

24

25

26

27

28

29

30

31

32

33

34

In WPP, as a rule, several industrial wind turbines are combined into a single network — the “wind farm” (WF) that is included in the unified energy systems. Currently, the basis for the development of industrial wind energy, including in Russia (Fortov, Popiel, 2014; Gordeev et al., 2012), are major WFs consisting of a large number of wind turbines. Sometimes they consist of up to 100 or more wind turbines. The rate of development of WF in Europe and America is currently comparable to that of nuclear energy development in the second half of the twentieth century, and might have even surpassed it already. Accordingly, the interest of modern scholars in rotor aerodynamics has significantly increased. Today, as in the productive aviation era of Joukowski and Prandtl and their schools, there has been a new phase of intensive scientific development of rotor aerodynamics (Okulov et al., 2013). It is primarily associated with solving the tasks of efficiency increase of wind turbines, arranged one behind the other and integrated in compact groups of WF. This requires additional optimization of work regimes of turbines that fall in the vortex wake behind the rotor of the preceding WF, where the deviation from the estimated optimal performance is due to a significant reduction of wind velocity inside the wake compared to the main flow. This velocity deficit and

* The work was financially supported by the Russian Science Foundation (Grant 14-19-00487).

35 an additional increase in the level of non-stationary pulsations due to interaction with vortex
36 structures coming off the rotor blades significantly worsen the working conditions of
37 subsequent turbines, falling in the wake in the farm (Vermeer et al., 2003). Average power
38 losses in a large wind farm make up from 10 to 20 % due to interaction with wakes of preced-
39 ing wind turbines. Therefore, the development of rotor aerodynamics today focuses primarily
40 on the study of the dynamics of vortex rotor wakes and the construction of new aerodynamic
41 models of interaction for the search for optimal configurations of WF (Sørensen et al., 2013).
42 These tasks are associated with the need to examine the far inter-rotor interaction. So far the
43 theory of rotor machines has been mostly considering the problem of near interaction between
44 the stator and rotor or two rotors for two-stage propellers, when the vortex system generated by
45 the blades of the first stage immediately interacts with the blades of the subsequent one.

46 New requirements to the description of rotor interaction at large distances in WF assume
47 addressing and solving more complex problems of classical aerodynamics related to the study
48 and description of complex swirling flows in the wakes, interactions with helical vortices and
49 their multiplets. It gives a new impetus to the study of fundamental problems in vortex
50 dynamics and the theory of stability of vortex structures (see, e.g., Okulov, Sørensen, 2007;
51 Walther et al., 2007; Felli et al., 2011; Quaranta, Leweke, 2015; Okulov, 2016). The need of
52 the industry in WF stimulated the development of some semi-empirical and engineering
53 methods of calculation of their work (Barthelmie et al., 2009; Larsen et al., 2013; Nygaard,
54 2014) even in the absence of exact concepts of the flow in the wake. As a result, the proposed
55 methods of calculation were limited to a different set of assumptions and all in all did not meet
56 expectations on their application for the development of the theory of wind turbines interaction
57 and for verification of numerical modeling.

58 Successful experimental investigation of new scientific problems posed by industrial
59 wind energy is practically impossible in full-scale wind turbines in the wind farm. Primarily,
60 this is due to the lack of reliable measurement techniques for studying a complex vortex system
61 of wakes at large distances behind the rotors of wind turbines under real atmospheric condi-
62 tions. In-situ atmospheric measurements are now limited to determining the wind velocity by
63 contact sensors at the measuring masts near the wind farm or non-contact laser velocimeters
64 (lidars, etc.) that are less reliable at great distances. The first ones allow estimating the velocity
65 profiles in a fixed position in space, along the mast, and the second ones measure some
66 averaged velocity values at different random points, but with a large error and not simultane-
67 ously, i.e., in different time intervals for subsequent averaging. Under undetermined atmo-
68 spheric pulsations, the obtained information on average values spread in time and space
69 becomes uninformative for subsequent analysis and generalization. So, today the priority role
70 in the experimental study of rotor interaction in FW still belongs to laboratory model studies.

71 Physical (laboratory) modeling in the development of rotor aerodynamics has always
72 been an effective research tool, since its formation in the early twentieth century. At that time,
73 the Russian aerodynamic school of Professor N.E. Joukowski, stimulated by the progress of
74 aviation, held leading positions in the world in the creation of rotary aerodynamics (Kuik et al.,
75 2015; Okulov, Sørensen, Wood, 2015). Today the interest of researchers has shifted from
76 aviation to the problems of wind energy, industrial development of which has been still
77 objectively delayed in Russia. Despite the obvious production lag, the Russian scientists
78 in their scientific research and development continue to obtain world-class results in this field
79 of knowledge. This is facilitated by two factors: the first, of course, is a huge theoretical
80 groundwork, created previously by the Russian school, and the second is problems with
81 the accuracy of field measurements, necessitating the development of fundamentals of aero-
82 dynamic interaction of wind turbines in the wind farms on the basis of the available laboratory
83 facilities. The current state of the studies results from to the lack of high-precision field mea-
84 surements. The lack of reliable field data has been compensated for the use of both domestic
85 and imported contactless high-precision laboratory measuring equipment in the model experiments.

86 It served to reveal important new patterns and to build theoretical models of aerodynamic rotor
87 interaction for optimizing the FW, which have made a significant contribution to the devel-
88 opment of the classical problems of rotor aerodynamics.

89 The aim of this review is to consider the role of modeling in the development of rotor
90 aerodynamics and to describe the most important results obtained in the last few years.

91 **1. The role of simulation in the development of rotor aerodynamics**

92 Theoretical studies on the rotor aerodynamics (marine propeller, propeller, wind turbine,
93 etc.) have always been accompanied by a simultaneous development of experimental
94 modeling. It should be noted that the first experience of such modeling was not very
95 successful. It was associated with testing the theory of the loaded disk — the simplest and
96 the oldest mathematical model of the propeller. In this abstract model, the load is replaced by
97 a uniform distribution of the pressure jump on the infinitely thin water-permeable disk, replac-
98 ing the rotor-swept area. The idea of such replacement dates back to the work of Rankine
99 (Rankine, 1865). A strict mathematical proof of the loaded disk action was found by Froude Jr.
100 (Froude, 1889), who showed that this theoretical model of the propeller/turbine has to
101 accelerate/decelerate the flow by one third before the disk, and by another third after it, with
102 a significant contraction/expansion of the wake behind the rotor for optimum operation
103 (the middle fragment, Fig. 1*a*).

104 Unfortunately, the experimental modeling at first did not confirm this simplest model of
105 an ideal propeller or turbine and led to its wrong interpretation, stating that behind the rotor
106 the fluid can neither speed up nor slow down, but flows in the form of an unperturbed
107 cylindrical column. Such misinterpretation was based on Parson's experiment, described in
108 the comments to the article (Froude, 1911). In fact, a nonexpanding or very slightly expanding
109 wake may be observed at partial loads on the rotor (Fig. 1*b*), and at normal or accelerated rotor
110 work, the wake expansion is well visualized (Fig. 1*c*). Perhaps, in the Parson's experiment,
111 the rotor worked at part-load, or a blocking effect appeared in the setup (Segalini, Inghels,
112 2014), distorting the flow behind the rotor. The misinterpretation of this experiment resulted
113 in a lag in the development of the rotor theory in England compared to the success of
114 the Russian and German scientific schools (Kuik et al., 2015).

115 In the early twentieth century, the first wind tunnels or water channels used simple
116 experimental methods and techniques: air visualization of the vortex structure behind
117 the propeller in the water, and determination of flow heterogeneities due to the deviation of
118 paper strips or filaments in the wake behind the rotor in the air. These were Flamm
119 visualization (Flamm, 1909) behind the propeller (Fig. 2*a*) and fixation of flow heterogeneity
120 behind the propeller by D.P. Ryabushinsky that formed the basis of N.E. Joukowski's
121 reasoning of the creation of the vortex theory of the marine propeller (Joukowski, 1912).
122 Successful interpretation of these model experiments enabled the formulation of the vortex
123 theory of the marine propeller (Fig. 2*b*) seven years before the German aerodynamic school of
124 L. Prandtl (Betz, 1919).

125 The vortex model of the rotor is now the main tool to study air and water propellers, wind
126 turbines, compressors, and turbines (Okulov, Sørensen, Wood, 2015). Moreover, it is the mo-
127 del that allowed showing the faultiness of the Parson's experiment and proving the correctness
128 of the Froude theory. Helical structure of tip vortices generates additional acceleration/dece-
129 leration of the flow in the wake behind propeller/turbine, which increases the flow deceleration
130 (Fig. 2*c*), associated with the selection of kinetic wind energy in the plane of the rotor.

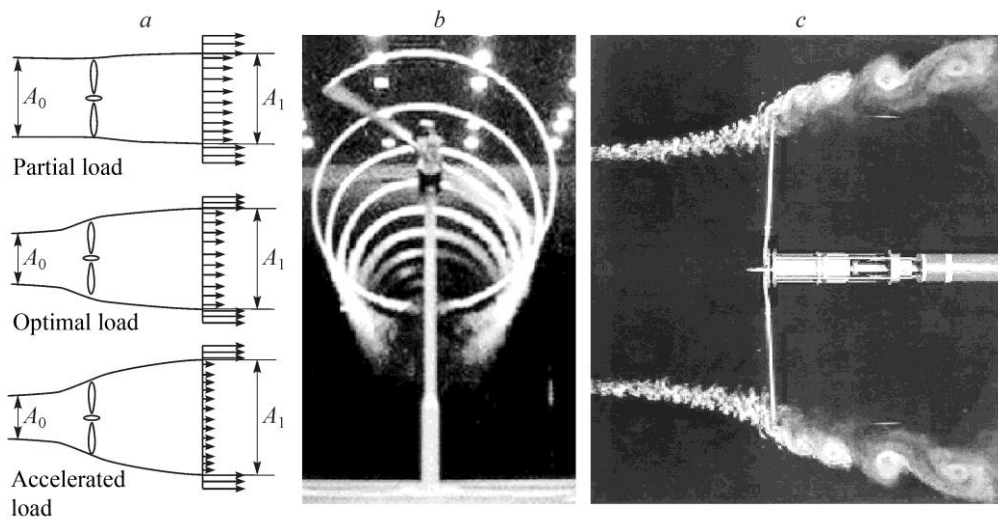


Fig. 1. Shapes of the wake behind the rotor.

a — schemes of flow development according to the jet theory of the loaded disk for different operation modes of the turbine (Hansen, 2008),

b — visualization of the mode of partial load without wake expansion (Hand et al., 2001),

c — visualization of the optimal operation mode of two-bladed rotor with flow tube expansion (Holten, 1981).

131 At optimum modes of the turbine operation, the deceleration doubles, which fully confirms
 132 the Froude theory.

133 The demand for laboratory testing today is due to a complex vortex structure of swirling
 134 flows behind the rotating impeller, requiring specific methods and techniques of research using
 135 modern high-precision measuring equipment (Okulov et al., 2007). In the wind energy,
 136 the more accurate measurements provide laboratory testing with a distinct advantage over
 137 in situ (field) measurements. As noted previously, the direct use of field tests is limited by
 138 the lack of reliable diagnostic tools for atmospheric currents. At large distances in FW it is pos-
 139 sible to fully study only the average flow characteristics in front of or in the wake behind the
 140 wind turbine rotor (Larsen et al., 2007), but the important information about the coherent
 141 helical vortex structure of the wake, which is well-fixed by visualization in the laboratory con-
 142 ditions, is lost with averaging (Figs. 1 and 2). Recently, the existence of a wake structure with
 143 helical tip vortices behind a full-scale wind turbine was effectively demonstrated in the unique
 144 full-scale experiment (Hong et al., 2014), carried out under special conditions. Thus, laboratory
 145 testing continues to play a decisive role, as for laboratory scale there are well developed
 146 measurement technologies that have been successfully used (Okulov et al., 2007).

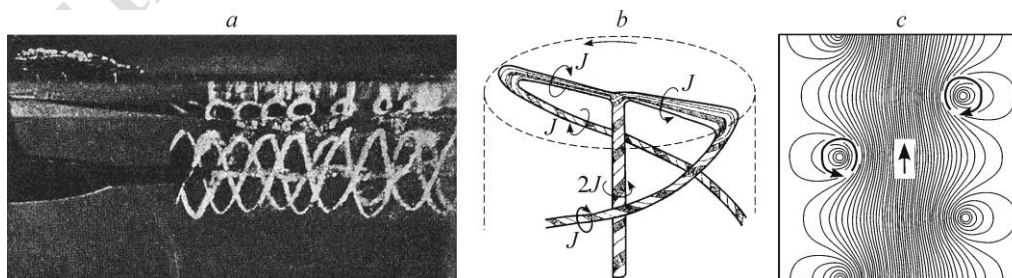


Fig. 2. Helical vortex structures.

a — visualization of the vortex structure behind the ship propeller in water (Flamm, 1909),

b — scheme of vortex model of rotor-propeller (Joukowsky, 1912),

c — structure of the flow induced by helical vortices, longitudinal section (Alekseenko et al., 2003).

147 Another argument in favor of the need for preliminary laboratory studies is associated
148 with separating the extraneous and external effects and eliminating the uncertainty of unique
149 atmospheric conditions of the experiment, which gives the opportunity to test different models
150 of rotor aerodynamics and to identify patterns of the rotor wake distribution. Laboratory mod-
151 eling in many cases is preferable to a direct field experiment, as it allows repeatedly reproduc-
152 ing the same inlet conditions on the rotor for the statistical set of data needed for processing
153 with a high degree of realizability. Therefore, it is advisable to start research on rotor inter-
154 action in FW from model experiments. Under in situ conditions, there are unpredictable effects
155 on the rotor and the wake mainly due to temporal and spatial non-uniformity of wind loading
156 and large-scale turbulence of the atmospheric boundary layer. In addition, currently because of
157 the growth in wind turbine size there are additional effects in blades streamlining. For example,
158 in their upper position, the wind velocity can reach 100 m/s, and to describe the aerodynamic
159 characteristics it may require consideration of compressibility, temperature stratification and
160 icing (Sunden, Wu, 2015) etc. In varying degrees, all of these perturbations are important, but
161 they are still secondary factors affecting the operation of wind turbines and complicating
162 the classical description of inter-rotor interaction, directly associated with the impact of rotors
163 and vortex wakes, generated only by the rotating blades of preceding turbine. From the first
164 half of the last century after the establishment of the foundations of classical vortex theory of
165 the propeller, in connection with an increase in flight speed and altitude, similar factors of
166 additional impact on the aircraft propellers have been taken into account in the form of correc-
167 tions. By analogy with the aviation development, for FW, the account for additional impacts
168 should become the next step after the establishment of the main regularities of wake
169 development and principles of their interaction with the subsequent turbine rotors. All addi-
170 tional factors should be studied after finding the basic patterns. They should be viewed as
171 perturbations of the initially established base models in order to assess the degree of each fac-
172 tor influence and to identify the need to take it into account or neglect it in "in situ" tests.

173 Another important question is the medium of modeling. For experimental verification of
174 the basic models and for the development of new models of the rotor in the early twentieth
175 century, in the period of aerodynamics formation, both air and water laboratory experiments
176 were quite successfully realized. In the modeling of low-speed propellers and turbines
177 (including wind turbines), the application of two different media is justified by the neglect of
178 compressibility due to small values of the Mach number. Even at velocities of 100 m/s, the cor-
179 rection for compressibility, which is proportional to the square of the Mach number, does not
180 exceed 9 %. However, sometimes there is unreasonable skepticism about modeling on water
181 for wind turbines due to significant differences in densities and viscosities of these media.
182 Indeed, locally there may be some differences, directly connected with solid streamlining and
183 boundary layer formation, but for a wide range of Reynolds numbers, their influence on
184 the wake formation behind blunt bodies is virtually absent (Sumer, Fredøse, 2006). Recently this
185 fact was confirmed in the wakes behind the rotating rotors, where in the experiments fluctua-
186 tions were discovered at close Strouhal numbers both in wind tunnels (Medici, Alfredsson,
187 2006) and in water channels (Chamorro et al., 2013; Okulov et al., 2014). The result in this
188 case depends on the correct scaling of the studied phenomena that has been repeatedly con-
189 firmed by comparison of similar data obtained in different media. For example, in the works of
190 N.E. Joukowski (Joukowski, 1912; Joukowski, 1914; Joukowski, 1915; Joukowski, 1918),
191 the vortex theory of the propeller was created based on Flamm visualization behind the pro-
192 peller in water, and was verified by experiments of D.P. Ryabushinsky with air propellers.
193 To study the rotor interaction of modern wind turbines the laboratory modeling in water
194 channels (Fraunie et al., 1986; Chamorro et al., 2013; Neary et al., 2013; Okulov et al., 2014;
195 Bachant, Wosnik, 2015) is often used for two reasons. First, for water it is easier to keep
196 the characteristic Reynolds number at small-scale simulation of wind turbines in small working
197 sections, limited by geometric sizes of wind tunnels (Treuren, 2015) and water channels.
198 Secondly, visualization and diagnostics of distributed characteristics in water have been

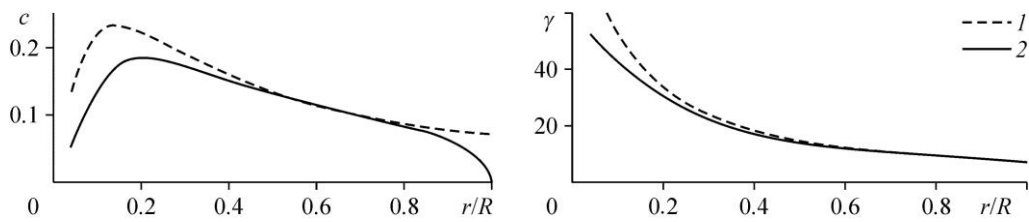


Fig. 3. The distribution of the chord c and the local pitch distributions γ for three-bladed rotor, built on BE/M method without adjustment for tip correction (1) and for exact solution on BE/LL-method with Goldstein circulation (2).

199 worked out much better and give more accurate results. Further, we will demonstrate several
 200 examples of such modeling and diagnostics for water that were successfully implemented with
 201 the participation of the author of this review. In the described studies, the identity of the ob-
 202 tained results was confirmed by their comparison in the two media.

203 2. Comparing the rotors of wind turbines constructed 204 using different optimization methods

205 The possibility of constructing the rotor blade through its separate elements cut with cy-
 206 lindrical sections, was considered by Drzewiecki in 1892 (Okulov et al., 2013). Using the pro-
 207 posed method, and in addition, to simplify the calculations, assuming that different flow tubes
 208 in each section behave independently from each other, Glauert calculated the parameters of
 209 the optimal rotor of the wind turbine (Glauert, 1935). He optimized equations of the pulse the-
 210 ory independently in each cylindrical flow tube, passing through the circular cross section, for
 211 any fixed value of the rotor radius, neglecting an existing interaction between them and
 212 the pressure changes in the radial direction. A method of “blade element/momentum” (BE/M)
 213 with different types of corrections for end effects is still the main tool in the design of rotors of
 214 wind turbines (Kuik et al., 2015). However, for modeling the blades, there is another vortex
 215 approach (Okulov, Sørensen, Wood, 2015). It is based on “blade element/lifting lines”
 216 (BE/LL). To determine the optimal distribution of circulation in BE/LL Goldstein (Goldstein,
 217 1929) applied the variational principle of Betz (Betz, 1919). In the rotor with such blade, or for
 218 short — in the Betz rotor, the distribution of circulation along the lifting line, replacing
 219 the rotating blade, shall provide for the coming down free vortex sheet to have a strictly helical
 220 form and to move uniformly in the axial direction. By analogy with the elliptic wing, such field
 221 of free vortices in the wake behind the rotor must meet its minimum inductive resistance and
 222 correspond to its optimum operation mode (Okulov, Sørensen, Wood, 2015).

223 In order to verify and compare the efficiency of rotors designed using different approa-
 224 ches (BE/M and BE/LL), a pair of identical three-bladed models, built on the original BE/M-
 225 method without correction for end effects and on the exact solution of the BE/LL-method with
 226 Goldstein circulation was experimentally compared (Okulov et al., 2015). The algorithm was
 227 developed for determining the form of blades for two rotors with the same impeller diameter
 228 $2R = 0.376$ m for the value of tip speed ratio $\lambda = 5$ ($\lambda = \Omega R/V$, where R is the radius of the ro-
 229 tor, Ω is the angular velocity of its rotation, and V is the free-stream velocity). Changes of
 230 the chord c for SD7003 profile (Selig et al., 1995) and a final angle of inclination in each sec-
 231 tion of the blades with a correction for the same angle of attack $\alpha = 4^\circ$ along the blades are
 232 shown in Fig. 3. In the design of the two blades, the influence of the rotor hub was neglected.
 233 For both rotors, it was the same, and this consequently led to the same influence. Note, howe-
 234 ver, that the question of the influence of the hub size on aerodynamic characteristics of wind
 235 turbines was studied separately. In the framework of the conducted research, it was established
 236 that for small hub ratios, typical of wind turbines, the influence of the hub on the aerodynamic
 237 characteristics of the rotor is negligible (Okulov, Sørensen, Shen, 2016), which is consistent with
 238 the conclusions made earlier at optimization of propellers (Wald, 2006). Both rotors were

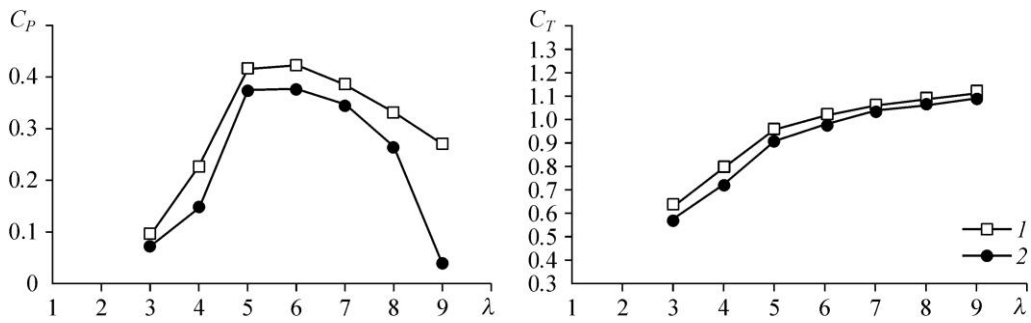


Fig. 4. The coefficients of power C_p and thrust C_T for Betz (1) and Glauert (2) rotors as a function of tip-speed ratio.

239 experimentally investigated in a water channel in order to compare their performance depend-
 240 ing on the tip-speed ratio. The question of the suitability of water channel or wind tunnel in
 241 this case was not relevant, since the experiment only meant to test two different philosophies of
 242 optimal design of the turbine blades, i.e., it was enough to compare different shapes of rotors,
 243 ensuring equal conditions of testing. Both models were placed in the channel at the operating
 244 temperature of 20 °C, the Reynolds number of about 240000, and the value of the oncoming
 245 flow velocity at the rotor location $U_\infty = 0.65$ m/s with its fluctuations not exceeding 3%. Pow-
 246 er characteristics of the model rotors were measured by strain gauge sensors, installed at
 247 the rotor mounting. Measurements were made for flow torque and thrust on the rotor for tip-
 248 speed ratios $\lambda = 3-9$. Figure 4 shows the corresponding dependences of power factors C_p and
 249 thrust C_T for both propellers. The maximum performance $C_{p_{max}}$ of both rotors was achieved at
 250 design tip-speed ratio of 5 and keeps its value up to $\lambda = 6$ (Fig. 4). For the first time, it was
 251 found that the three-bladed rotor of Betz built exactly on the vortex method BE/LL allows ob-
 252 taining more kinetic energy from a uniform incoming flow.

253 Along with the experiment, a comparison of the shapes of blades took place; some of
 254 them were obtained by calculation as a result of applying BE/LL-method and others were ob-
 255 tained by other designing approaches, including consideration of the continuous distribution of
 256 circulation along the blades — NEJ rotor (Joukowsky, 1912; Joukowsky, 1914), and the limit-
 257 ing cases of infinite number of blades. More detailed information about various models may be
 258 found in reviews (Kuik et al., 2015; Okulov, Sørensen, Wood, 2015), as well as in the book
 259 (Sørensen, 2016).

260 The works (Sørensen, 2016; Sørensen et al., 2016) compared the shapes of the blades,
 261 constructed analytically in accordance with different theories. Figure 5 shows the results of

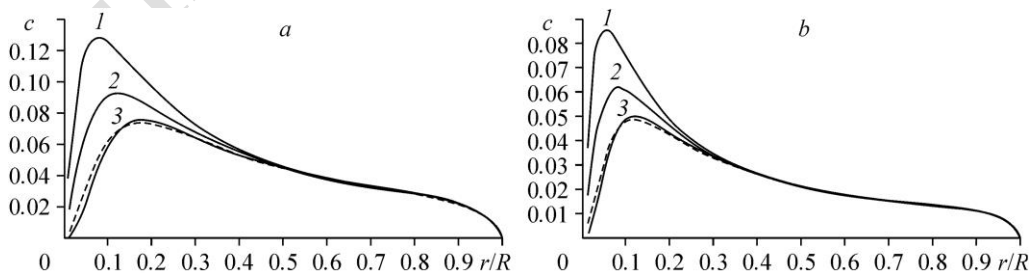


Fig. 5. The change of the chord c along the blade r/R for tip-speed ratios $\lambda = 6$ (a), 9 (b) in the calculating of the blade shape by different simulation methods.

Solid lines — approximations on model with an infinite number of blades with correction for the number of blades on Prandtl correction (Sørensen, 2016):
 1 — BE/LL with constant circulation NEJ, 2 — BE/M, 3 — BE/LL with Goldstein circulation;
 dashed line — accurate calculation on BE/LL for three-bladed rotor of Betz (Sørensen et al., 2015).

262 comparison of different geometries of the blades, constructed with different approaches for
263 turbines with different tip-speed ratios. For a more correct comparison, the correction for
264 the end effect of the blade was applied to approximate models with infinite number of blades.
265 The effect of different methods of correction of the blade tip shape, starting with the first cor-
266 rection proposed by Prandtl (Betz, 1919), was investigated in the work (Wood et al., 2016).

267 Figure 5 shows that the blades designed by BE/M or different approximations on BE/LL
268 method, after additional end correction of Prandtl, model the blade tip in very good agreement
269 with the Betz rotor, constructed on the exact BE/LL solution for a finite number of blades and
270 Goldstein circulation. The comparison shows that the geometry of the blades depends on the
271 calculation method, but the differences mostly exist in the axial part of the blade and become
272 significant for small values of a turbine tip-speed ratio, limited by value of 5. The design of
273 an optimal blade was further refined by taking into account the nonlinear influence of tip vortices
274 (Wood, Okulov, 2017). As a result, a negligible impact of this additional non-linear correction
275 on baseline BE/LL solution was found; moreover, it arose in a very narrow range for even
276 smaller values of tip-speed ratios from 0.8 to 1.5. Note that wind turbines typically operate at
277 much greater tip-speed ratios, starting from 5 and above. Therefore, approaches to
278 the construction of the blades, based on ideal models with an infinite number of blades in com-
279 bination with the use of corrections for end effects (Wood et al., 2016) lead to practically iden-
280 tical geometries of the end blades. They are still very close to the shape of the blade, defined by
281 the exact BE/LL solution for Betz rotor with a finite number of blades (Okulov, Sørensen,
282 2008; Okulov, Sørensen, 2010b). This important conclusion partly explains why the earlier
283 practice of using approximate models in the design of the blades was so effective. However,
284 the question on the role of differences in axial forms of blades on the performance of wind tur-
285 bines remains unanswered yet. The most significant is this difference for Betz and NEJ rotors
286 (Fig. 5, curves 1 and 3), and further investigation requires an additional experimental testing.
287 Interest in this issue is warmed up by the discussion about the possibility to obtain a larger ki-
288 netic energy of the wind by NEJ rotor compared with the Betz rotor; it is based on analytical
289 study of different limiting models with an infinite number of blades for small tip-speed ratios
290 (Sørensen, Kuik, 2010). Recent theoretical study (Kuik, 2016) once again established the supe-
291 riority of the NEJ rotor, but again, in an unrealizable ideal limiting case with infinite number of
292 blades. The answer can be obtained only after experimental comparison of the Betz and NEJ
293 rotors with a finite number of blades.

294 3. Studying the wake behind the disk in water channel and wind tunnel

295 Before proceeding to the modeling and study of the development of rotor wakes, let us
296 investigate the properties of self-similarity in the wakes behind bluff bodies, in this case behind
297 the disk in different media: in air and water ones. To describe the wake behind the disk in
298 water such testing was conducted in the work (Naumov, Litvinov et al., 2015). With the help of
299 measurements made by digital tracer visualization (PIV) and laser Doppler anemometer
300 (LDA), the regularities of attenuation of the axisymmetric turbulent wake behind a stationary
301 disk in a water channel were investigated, and a comparison with the experiments performed
302 earlier with the comb of thermoanemometers behind the stationary disk in a wind tunnel was
303 realized (Johansson, George, 2006). In a turbulent axisymmetric wake behind the disk, the pro-
304 perty of self-similarity (self-similarity of velocity profiles) was tested; it has to manifest and
305 should be sustainably reproduced in a wide range of Reynolds numbers, covering the regimes
306 of operation of real wind turbines. It seemed interesting in each cross section of the wake be-
307 hind the disk at a distance x for different media to compare the form of dimensionless profiles of
308 velocity deficit $(U_\infty - U(r))/U_0$, where U_∞ is the freestream velocity, $U_0 = \max(U_\infty - U(r))$
309 is the velocity deficit on the wake axis, and U is the profile of the longitudinal velocity

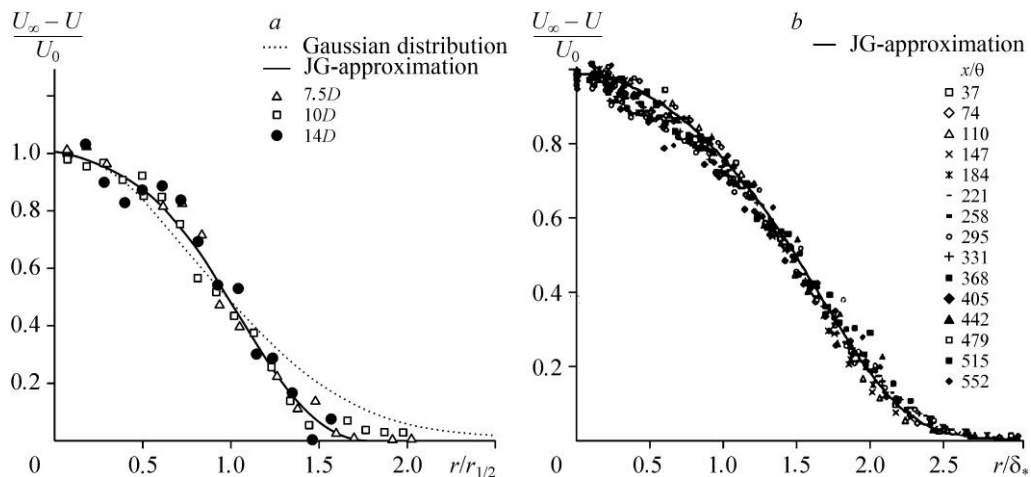


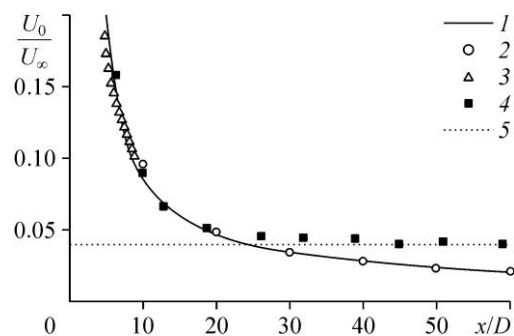
Fig. 6. Testing self-similarity of velocity profiles in the wake behind the disk.

a — water channel with profile width normalization at the point of half-value of the deficit (Naumov et al., 2015),
 b — wind tunnel normalized by the profile width (Johansson, George, 2006).

310 component. For profile description, the JG-approximation $(1+ar^2+br^4)e^{(-cr^2-dr^4)}$ with fixed
 311 parameters $a = 0.049$, $b = 0.128$, $c = 0.345$, and $d = 0.134$ proposed in (Johansson, George,
 312 2006) (Fig. 6b, the distance between the profiles and the disk $x/\theta = 552$ corresponds to $150D$)
 313 was used. JG-approximation differs slightly from the usual Gaussian distribution, but better
 314 models the wake in both tests (Fig. 6) both behind the disk in the water channel and behind
 315 the disk in the wind tunnel, for small Reynolds number $Re = 2 \cdot 10^5$ and $Re = 2.6 \cdot 10^4$,
 316 respectively, falling within the range of existence of the self-similar wake.

317 Another important issue is to clarify the influence of the medium phase state on
 318 the attenuation of the velocity deficit in the wake along the disk axis downstream. This
 319 attenuation behind the disk in the water channel coincided with a rational dependence
 320 $0.32(x/D - 3.2)^{-2/3}$, established in earlier experiments in the air in the wind tunnel (Johan-
 321 sson, George, 2006) (Fig. 7). The Figure shows that at points of the far wake ($x/D \geq 5$), there is
 322 a monotonous decay of deceleration with a degree of $-2/3$ approaching the asymptotic
 323 horizontal line at $x/D \geq 25$, which determines the level of background fluctuations in the on-
 324 coming flow below which the existence of a wake is impossible to distinguish. Note that
 325 the deceleration rate of the wake behind the disk in the water channel coincided with its
 326 attenuation behind the disk in the wind tunnel despite the above differences in Reynolds
 327 numbers. Indeed, for a wide range of relatively large Reynolds numbers, the degree of $-2/3$ for
 328 turbulent axisymmetric wake attenuation remains behind any blunt axisymmetric body
 329 (George, 1989; Novikov, 2009). For small,
 330 subsonic flow velocities it does not depend

Fig. 7. A comparison of attenuation of velocity deficit behind the round disk in the water channel and the wind tunnel.
 1 — a power dependence with exponent of $-2/3$,
 2 — measurement in the air (Johansson, George, 2006), measurement in water:
 3 — PIV technique, 4 — LDA method,
 5 — the level of external disturbance in the water channel (Naumov et al., 2015).



331 on the medium (water or air). In addition, it has been recently discovered that the degree of
332 attenuation of the wakes remains at their non-axisymmetric streamlining as well (Jiang et al.,
333 2016). Data presented in the paper (Naumov et al., 2015) confirm the universal properties of
334 self-similarity and attenuation of a far turbulent wake at relatively high Reynolds numbers and
335 the possibility of their studies in water channels and wind tunnels.

336 **4. Comparing the wakes behind the rotor and the disk**

337 The prediction of the operation mode of the wind turbine falling in the wake from
338 the previous turbine, is fundamental for calculating losses and optimizing the wind farms.
339 To solve this problem it is necessary to create an adequate model of the wake development
340 behind the rotor. Today, the most popular are the kinematic models based on self-similarity
341 profiles of velocity deficit at the conservation of mass and momentum in the wake, which use
342 the assumption of a linear wake expansion and the experimental value of the coefficient of
343 flow thrust on the swept surface of the wind turbine rotor as input data. It should be noted that
344 the assumption of a linear wake expansion and conservation laws uniquely determine the wake
345 attenuation according to the hyperbolic law with the exponent of -1 , which differs from
346 the above considered case of its attenuation behind the blunt bodies with index $-2/3$. Although
347 there has been no purposeful experimental study of wake development behind wind turbines
348 for sufficiently large distances, a priori applied in practice is the model of Jensen (Jensen,
349 1983) with wake attenuation coefficient of -1 or its modifications, specifying only the shape of
350 the velocity deficit profiles in the wake. For example, in (Bastankhan, Porte-Agel, 2014),
351 it was proposed to use a Gaussian distribution. The next step of the research was a more
352 thorough examination of the law of deceleration of the far wake behind the rotor.

353 An overall idea of the flow structure behind the rotor operating in turbine mode has been
354 long known. Taking the energy of the incoming flow, the turbine rotor slows it down, forming
355 a characteristic velocity gap in the wake — the deficit characteristic of the wakes behind bluff
356 bodies. The fundamental difference between the wakes for blunt bodies (in our consideration,
357 disks) and rotors should be noted as well. In the first case, the flow deceleration is due only to
358 the resistance of the body and has a passive character. In contrast, the flow deceleration behind
359 the rotor is a result of its active influence and is associated with kinetic energy removal from
360 the flow. In the rotor plane, the flow is decelerated by the useful energy removal. At optimal
361 mode, the deceleration in it is about $1/3$ of the initial velocity, but it is not finished and further
362 occurs already in the wake. The velocity is additionally reduced by one more third, and total
363 deceleration reaches $2/3$ of the unperturbed velocity.

364 In the near wake, when the effect of the turbine on the flow is over, additional braking is
365 determined by the impact of the system of helical vortices (Fig. 8a), coming off the ends of
366 the blades. They generate one more flow along the axis (Fig. 2c), which further slows the flow.
367 Such flows do not exist in the wake behind the disk (Fig. 8b). Behind the rotor, such additional
368 deceleration is registered in all the dimensions of velocity profiles of the near wake (Naumov
369 et al., 2012; Naumov et al., 2014). Its growth completely stops at a distance of 2–4 diameters
370 of the rotor, when the vortex system is completely destroyed and its effect is over.

371 Additional deceleration of the averaged velocity profiles in the near wake was also
372 repeatedly registered in different field experiments (Vermeer, Sørensen, Crespo, 2003).
373 However, there was some skepticism about the possibility of using data of model studies on
374 the influence of helical tip vortices on the formation of the near wake behind real wind
375 turbines, because their existence could not be fixed in situ by any available means of
376 measurements in the atmosphere (Larsen et al., 2007). The authors of (Hong et al., 2014)
377 undertook a unique field experiment, where the original solution, namely the use of snowflakes
378 for the tracers in large-scale PIV-measurements in the near wake behind a 2.5 MW wind
379 turbine, served to clearly determine the existence of concentrated tip vortices, predicted
380 in many air and water model experiments.

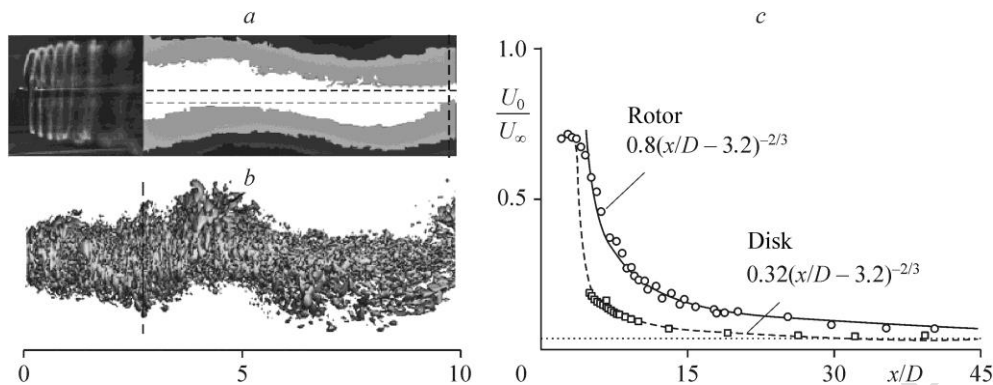


Fig. 8. Comparison of the wake structure.

The wake over the active rotor (Okulov et al., 2014) (a), passive disk (Yang et al., 2014) (b); a comparison of the attenuation of velocity deficit in both wakes (Litvinov et al., 2016) (c).

381 Termination of the effect of tip vortices in the wake is due to their destruction, as the full
 382 vortex system in combination with a central axial vortex (Fig. 2b) is absolutely unstable
 383 (Okulov, Sørensen, 2010a; Felli, Camussi, Di Felice et al., 2011). Behind the rotor at distances
 384 over its 2–3 diameters, helical vortices are destroyed (Fig. 8a) and their effect on the flow is
 385 stopped. Formation of the long wake starts after the destruction of the near wake and
 386 the maximum braking at a distance from 2 to 5 diameters from the rotor. Behind the near wake
 387 (highlighted area in Fig. 8a and 8b), first, the far wake both for the rotor and the disk
 388 similarly forms into a large helix. The comparison of the dynamic characteristics of the wakes in this
 389 region has revealed the development of low frequency oscillations at constant Strouhal number,
 390 the well-known phenomenon at streamlining of a blunt body (in this case, the disk) that is
 391 reproducible in a wide range of Reynolds numbers. In addition, for the first time for rotor,
 392 the work by (Okulov et al., 2014) established a weak dependence of the frequencies of these
 393 oscillations on the parameter of tip-speed ratio of the rotors for optimal and accelerated loads.
 394 This is because at rapid rotation, the surface swept by the rotor acts similar to an impermeable
 395 disk at the forming of the shape and dynamics of low frequency oscillations of the far wake.
 396 Note that the presence of low frequency oscillations at Strouhal frequencies was established
 397 in the wakes behind the rotors for both media: in experiments in the air in the wind tunnel, this
 398 frequency was recorded in (Medici, Alfredsson, 2006), and a full-scale study in the water
 399 channel was conducted by the authors (Okulov et al., 2014). As a result, once again, the cor-
 400 rectness of the modeling of the dynamic development of the wake in both media was con-
 401 firmed.

402 In experiments (Okulov, Naumov et al., 2015), the similarity of the far wake behind
 403 the active rotor with the wakes behind the passive fixed blunted bodies, disk or sphere, was
 404 also observed in their further development. The purpose of the work (Naumov, Mikkelsen,
 405 Okulov, 2016) was the creation of an experimental model of the wake behind the wind turbine
 406 rotor to assess the maximum distance of its propagation. In Fig. 8c, a solid line shows a curve
 407 approximating a change in average axial velocity in the far wake of the rotor depending on
 408 the distance from it. The far wake starts forming after the destruction of the near wake and
 409 the reaching of its maximum braking behind the rotor at a distance from 2 to 5 diameters.
 410 Additionally, Fig. 8c shows a comparison of the above data with the data for the wake develop-
 411 ment behind a disk. Their comparison has shown that the attenuation of the far wake in both
 412 cases follows the same power law differing only in the intensity of velocity deficit in
 413 the wakes, which is reflected in the coefficients at equal power dependence of attenuation
 414 (Fig. 8c). In the wakes behind the rotor, this relative ratio of attenuation intensity has a much
 415 larger value (0.8) compared to the value behind the disk (0.32). The differences in the inten-
 416 sities of velocity deficit are understandable. Thus, in contrast to the passive flow deceleration

417 behind the disk, the rotor actively influences the incoming flow, transforming its energy into
 418 torque, and, in addition, extra deceleration is generated by helical tip vortexes.

419 Note that the self-similar behavior of the far wake was independently established
 420 in different sections behind the rotor of the wind turbine in the water channel (Okulov,
 421 Naumov et al., 2014) and wind tunnels (Dufresne, Wosnik 2013; Bastankhan, Porte-Agel,
 422 2014). The authors of the latter two works showed self-similarity of the wake behind the rotor,
 423 but due to an insufficient length of the measuring section, small values of the rotor tip-speed
 424 ratio and lack of precision of air measurements in these works, the values of the coefficients in
 425 the laws of attenuation were difficult to establish exactly. The data of the testing of self-
 426 similarity of the wake behind the rotor in the water channel (Okulov, Naumov et al., 2015),
 427 presented in Fig. 9, showed a good agreement of the shapes of profiles in the wake and JG-
 428 approximation proposed to describe the wake behind the disk by the authors of (Johansson,
 429 George, 2006) and previously used to analyze the data in Fig. 6. In addition, the authors
 430 (Okulov, Naumov et al., 2015) first discovered and described the presence of the same self-
 431 similarity for different tip-speed ratios of the rotor (Fig. 9b). The difference occurred only for
 432 slow rotation of the rotor $\lambda = 2$ (with a design optimum at $\lambda = 5$), when the approximating
 433 function was closer to a Gaussian distribution rather than to JG-approximation.

434 Thus, the behavior of the far wake behind the rotor was to a large extent identical with its
 435 behavior behind the disk, starting from the occurrence of low-frequency oscillations at Strouhal
 436 frequency, weakly dependent on the change of the Reynolds number and ending with the wake
 437 self-similarity with the same degree of attenuation with exponent of $-2/3$, but with different
 438 intensity factors. At conservation of mass and momentum in the wake, this attenuation
 439 determines the power law of its expansion with exponent of $1/3$, i.e., the real behavior of
 440 the wake differs from the used kinematic models with linear expansion (Jensen, 1983;
 441 Bastankhan, Porte-Agel, 2014; Bastankhan, Porte-Agel, 2016). Consequently, the use of
 442 kinematic models with a linear expansion of the wake is not entirely correct and can probably
 443 only be successful at its short segments, where a linear approximation is performed for a wake
 444 really expanding according to a different law. One more simplified modeling may be realized,
 445 apparently, by determining the similarity of the behavior of the far wake behind the disk and

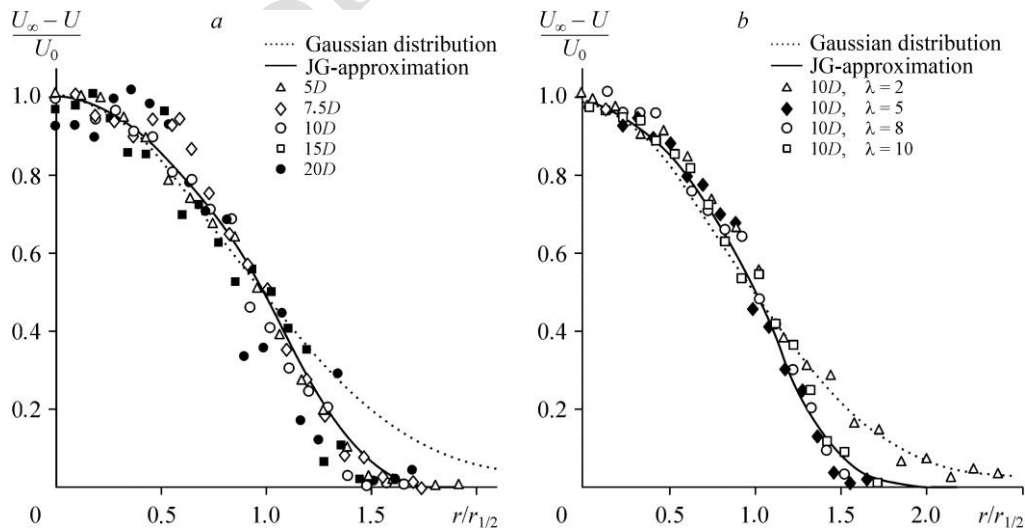


Fig. 9. Examining self-similarity of velocity profiles in the wake behind the three-bladed rotor depending on the distance behind the rotor (a) and on its tip-speed ratio λ (Okulov et al., 2015) (b).

446 the rotor. For example, in the calculation of the wind farms for ease it would be convenient to
 447 replace the rotors by simpler disk models, using the formal correction of the wake intensity
 448 ratio from 0.32 to 0.8 or correcting the thrust coefficient, as in the model of Jensen (Jensen,
 449 1983), but, of course, within the discovered power law of $-2/3$. These possibilities will be
 450 discussed in the next Section.

451 **5. The aerodynamic interaction of the rotors and disks**

452 Before describing the modeling results let us refer to the data of operation of the real
 453 wind farm “London Array” (Nygaard, 2014), presenting the results of power generation in four
 454 different combinations of wind turbines, located in the wakes behind each other at frontal wind
 455 directions. In one case, it was expedient to choose two chains F20-F01 and J20-c J06 with
 456 wind direction of 312.2° and spacing between turbines of $5.4D$ rotor diameters, and in the se-
 457 cond, C19-M19 and A13-L13 with wind direction of 222.3° and spacing of $8.3D$. Changes of
 458 the wind power removed by turbines along the chains in relation to the performance of the first
 459 turbine in the chain are shown in Fig. 10a and 10b, respectively. The work of three chains of
 460 the four is characterized by the effect of stabilization of the energy removed from the wind or
 461 power produced by turbines. In the fourth chain (A13-L13), power is not stabilized but
 462 continues to fall from turbine to turbine, which is consistent with the classical idea of reducing
 463 the velocity of each turbine, at least by one-third, which naturally reduces the power of turbine
 464 falling in the wake of the next turbine and further throughout the chain.

465 Precise explanation of the stabilization effect in the turbine chain operating in the wakes
 466 of one another has not been found yet, although this effect is well known and is used
 467 in the operation of wind farms. The lines in graphs of Fig. 10 present the results of calculations
 468 on Jensen model at its local application and sequential transition from one turbine to another;
 469 every time the specifically measured thrust coefficient was used for the calculated turbine.
 470 Note that this step-by-step empirical correction describes well the effect of stabilizing
 471 the energy removed from wind by the wind farm that is expected due to correlation between
 472 generated power and wind thrust on the surface swept by the rotor, used as an empirical
 473 parameter of the model. That is the model of Jensen and its variants (Jensen, 1983;
 474 Bastankhan, Porte-Agel, 2014; Bastankhan, Porte-Agel, 2016) due to their empiric nature can-
 475 not clarify the reason for the stabilization effect, which is obviously associated with the re-
 476 covery of velocity profile before the next turbine in the chain. In addition, these models do not

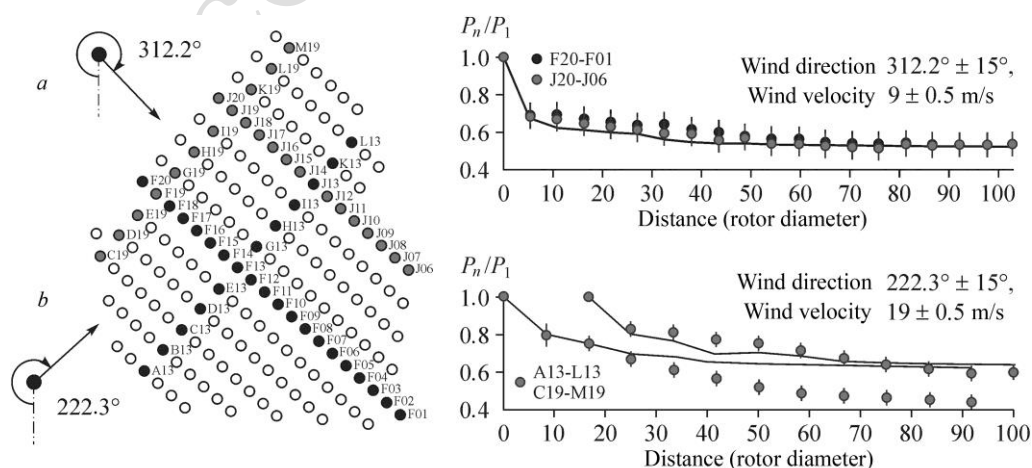


Fig. 10. Effect of stabilizing the energy taken from the wind in selected chains of wind turbines in the wind farm “London Array” (Nygaard, 2014).

477 always accurately describe the actual operation of the wind farm (for example, for the mode in
 478 Fig. 10b). Here, significant are the remoteness of turbines in the wind farm providing a greater
 479 velocity deficit; the atmospheric turbulence responsible for more intense mixing; the non-
 480 uniformity of the velocity profile of the incoming flow or, more likely, the simultaneous
 481 impact of all factors affecting the recovery of the velocity profile in the wake. Of course, for
 482 a correct description of the phenomenon, it is useful to estimate the degree of influence of each
 483 factor on the studied effect, but, as mentioned earlier, today it is impossible to do in situ
 484 because of the lack of precision of the measuring techniques and the uncontrol-lability of
 485 natural conditions in the FW operation for eliminating certain factors. Thus, once again we
 486 return to the need for modeling, which can begin with the study of the interaction between two
 487 turbines in conditions of practical absence of external turbulent fluctuations and the non-
 488 uniformity of the profile of the incoming flow. Such an idealized modeling of working
 489 conditions will allow obtaining information about the basic interaction of the rotors to further
 490 add other disturbances and assess their individual impact on the system performance.

491 The study by (Okulov, et al., 2017) used two identical models of horizontal wind turbines
 492 (Fig. 11a). In sections 2 and 4, a single model of such rotor was used to study its strength
 493 characteristics and the wake behind it in the water channel. In the experiments, the rotor fre-
 494 quencies n and the distance between them H varied. Depending on the fixed values of these
 495 parameters, on the measured values, the power factor and the thrust coefficient were calculated
 496 for both rotors. It should be noted that determining the tip-speed ratio of the second rotor was
 497 more difficult compared to the first rotor since the velocity of the incident flow on the second
 498 rotor was not known in advance and could not be used in a definition of the tip-speed ratio.
 499 There were also problems due to uneven profile of the incoming flow velocity in accordance
 500 with JG-approximation of the wake behind the first rotor. However, the authors managed to
 501 establish a simple relation for estimating the maximum efficiency of the second rotor. It turned
 502 out that changing the power output of the second rotor, related to the first one's power,
 503 depending on the distance between them can be estimated using the law of wake atten-
 504 uation behind a single rotor as a square of velocity change on its axis: $(U_0/U_\infty)^2 =$
 505 $= (1 - 0.8(x/D - 3.2)^{-2/3})^2$ (Fig. 11b). The figure presents not only the data of experiments in
 506 the water channel, but also the results of the experiments in the wind tunnel, which once again
 507 confirm the identity of modeling in different media. The latest data are represented by a single
 508 point because the dimensions of the working section of the wind tunnel did not allow making
 509 the distance between the rotors over $5D$. In addition to the study of rotors arranged on the same

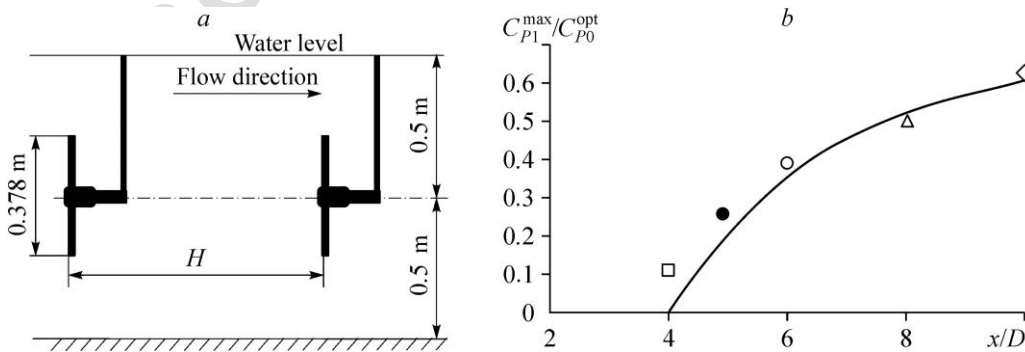


Fig. 11. The interaction between the two turbines.

a — scheme of setup, b — ratio of the maximum power of two rotors depending on the distance between them $H = xD$: bright characters — experiments in the water channel (Okulov, et al., 2017), dark character — experiments in the wind tunnel (Bartl et al., 2012), solid line — the square of the relative velocity on the axis of the wake behind a single rotor.

510 axis, the work (Okulov et al., 2017) studied the cases when the axes were shifted by half and
 511 by a full diameter. Nothing unexpected was found, and the worst was the case of rotors
 512 arrangement along the same axis when the second one fell completely into the wake of the first
 513 one.

514 Of particular interest is the study of the development of the far wake behind the second
 515 rotor and, accordingly, a comparison of its behavior with the wake generated behind two disks
 516 in the same configurations.

517 A comparison of the wake development at streamlining of passive systems with two im-
 518 movable disks and behind two active rotors (Fig. 12a) has revealed a fundamental difference
 519 between them (Naumov, Litvinov, et al. 2016; Okulov, Mikkelsen et al., 2016; Okulov,
 520 Litvinov et al., 2017a; Okulov, Litvinov et al., 2017b). In particular, the introduction of
 521 the second disk in the wake of the first one causes an increased deceleration in a total wake,
 522 which is natural for passive systems and is related to the emergence of additional resistance of
 523 the second disk, increasing the initial braking and the total intensity of the wake. In contrast,
 524 the deceleration in the wake behind two active rotors decreases. A typical approach to explain-
 525 ing different features in the wake development is a reference to the difference in turbulence
 526 characteristics. However, in the considered experiments for all wakes, behind single and
 527 double passive and active systems, the distribution of the pulsations intensity was almost
 528 the same (Fig. 12b). Therefore, we can assume that the turbulent characteristics may not be
 529 the main reason of the established phenomenon.

530 The recorded difference in the behavior of the wakes behind passive and active systems is
 531 a crucial result, as the found decrease in the intensity of the wake behind the two rotors can
 532 become the key to unraveling the effect of stabilizing the power generated by the chain of wind
 533 turbines. To understand the unexpected fact, i.e., the decrease in the intensity of the wake be-
 534 hind two working rotors as opposed to its growth for two disks, let us recall the difference
 535 in the formation of the wake behind active and passive systems. As mentioned earlier, a strong
 536 influence on the formation of the wake behind the rotor is exerted by helical vortex system
 537 of tip helical vortices (Fig. 2 and Fig. 8a), providing an additional doubling of velocity deficit
 538 in the wake. It is reasonable to assume that the vortex system in the wake of the first rotor
 539 destroys the system of the second one, leveling its contribution and reducing the intensity
 540 of the total wake. Of course, this assumption should become the subject of comprehensive
 541 examination in further studies.

542 Indeed, the influence of large-scale pulsations in different wakes on the performance
 543 of turbines falling into them is not well understood yet. This fact is also confirmed by the study

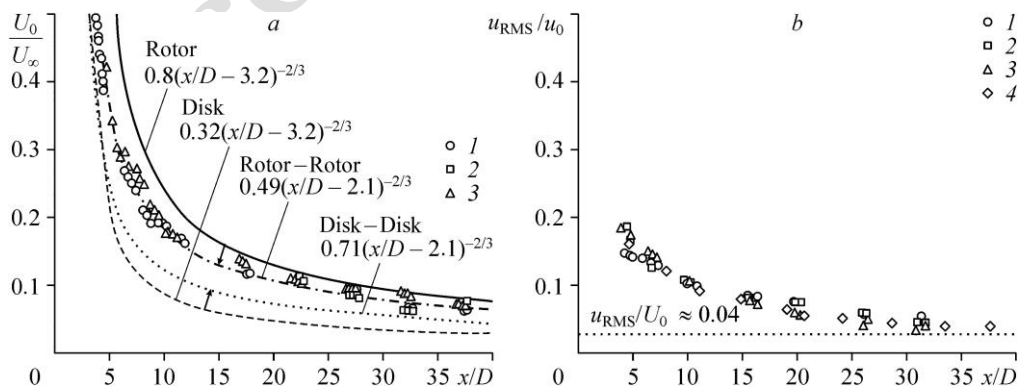


Fig. 12. Comparison of the far wake behind the single or double systems of rotors and disks.

a — velocity deficit attenuation: $H = 4D$ (1), $6D$ (2), $8D$ (3),
 b — development of turbulent pulsations (Okulov, Mikkelsen et al., 2016):
 $L_x = 4D$ (R-R) (1), $6D$ (R-R) (2), $8D$ (R-R) (3), D , $D-D$ ($L_x = 4D-8D$) (4).

544 of the effect of the wake from obstacles (disk) on the operation of the wind turbine (Naumov
545 et al., 2016; Naumov et al., 2017). It is shown that at different positions of the obstacles rela-
546 tive to the axis of the rotor, the velocity deficit in the section in front of it ranges from 0
547 to 20 %, and the level of turbulence coming from the obstacle has always been high: from 8
548 to 15 % compared to 4 % of the background value in the free stream. It has been found that
549 the capacity of wind turbine is affected only by its falling in the zone of the shadow from
550 the wake behind the obstacle, and the increase in pulsations has almost no effect on the power
551 level, which also requires a more careful study.

552 **Conclusion**

553 This retrospective review on the development of scientific bases of rotor aerodynamics
554 (Kuik et al., 2015; Okulov, Sørensen, Wood, 2015; Fukumoto et al., 2015) has revealed
555 the determinant role of laboratory testing in the study of the wind turbine operation. The role of
556 these studies for modern solutions of wind power problems has been determined. Return to
557 laboratory testing at the present stage of development of rotor aerodynamics, as well as
558 previously, is due to the impossibility of a full-fledged field study because of the complex
559 nature of inter-rotor interaction in FW, the lack of sufficient precision and absolute irreproduc-
560 ibility of natural conditions, which substantially complicates common patterns and concepts in
561 the field experiment. For the laboratory testing, it was necessary to analyze, adapt and further
562 develop various precise methods for measuring the kinematic characteristics of fluid motion,
563 using optical laser methods in the wakes behind the models of wind turbines with
564 the dominance of helical vortex structures and their subsequent collapse and formation of
565 the far wake. Using modeling it became possible to answer questions on the design of turbine
566 rotors and to determine the regularities of the wake development and inter-rotor interaction.
567 The effectiveness of different forms of turbine rotors based on various classical optimization
568 techniques has been so far compared only at modeling. As a result, the larger performance has
569 been revealed in the rotor designed in accordance with the concept of Betz (Okulov, 2014) and
570 the distribution of Goldstein circulation along the blade (Okulov and others, 2015). It should be
571 noted that various approximate methods of designing blade shapes with the use of different
572 corrections on the impact of the blade ends (Wood et al., 2016) give good approximation to
573 the shape of the optimal blade. With a slight influence of rotor hubs of small size (Okulov,
574 Sørensen, Shen, 2016), these forms differ only when approaching the rotor axis (Sørensen
575 et al., 2016), which indicates the high efficiency of existing wind turbines, the rotors of which
576 were designed by various approximate optimization methods.

577 The priority fact discovered in the study of the development of the far wake behind
578 the rotor is the detection of a uniform analytical model to describe its self-similarity and decay
579 according to the power law with the exponent of $-2/3$ (Naumov et al., 2016). The identified
580 model turned out to be suitable for arbitrary modes of the rotor operation in the modeling of
581 the far wake formed in the breakup of the helical vortex structure of the near wake (Naumov
582 et al., 2014). For different parameters of the wind turbine model operation, regardless of
583 the structure of the near wake and forms of its collapse, the far wake always formed with the
584 same structure, except for the modes of very small tip-speed ratio, not implemented in practice
585 (Okulov, Naumov et al., 2015). The same structure of the far wake was produced in the case
586 when the near wake consisted of inner and outer rings of helical vortices, descending
587 simultaneously from hub and tip edges of the blades. The possibility of these modes to exist
588 was seen repeatedly in experiments and was proved in theory as the existence of equilibrium
589 states for internal and external helical vortices (Okulov, 2016).

590 An important stage in the presented review was to determine the influence of the wake of
591 a preceding turbine on the performance of the following wind turbine. For distances between
592 the turbines exceeding four calibers (on rotor diameter), a simple relationship has been found
593 to determine the losses of the second wind turbine depending on its distance (Okulov, et al.,

594 2017). Of particular interest is the comparison of the behavior of wakes behind the separate
595 rotor and the system of two rotors, arranged one behind the other. The recorded sudden
596 decrease in the wake intensity behind the two rotors can be the key to unraveling the effect of
597 stabilizing the generated power in the chain of wind turbines (Okulov, Naumov et al., 2016).
598 Additionally, these experiments showed that the system of two disks can not satisfactorily
599 replace the system of two rotors, for example, to simplify calculations, as in the first case,
600 the total intensity of the wake increases, and in the second, decreases compared to a wake be-
601 hind a single disk or rotor, respectively.

602 In the study of the influence of the wake of a large-scale obstacle, it was found that
603 the capacity of wind turbines is affected by its presence in the zone of the wake shadow behind
604 the obstacle, and the increased pulsations due to the presence of heterogeneity almost did not
605 affect the operation of the wind turbine (Naumov et al., 2016). Certainly, further studies of
606 the effects of different disturbing factors should be extended to stratified flows (Voropaeva
607 et al., 2016) that model the natural non-uniformity of the atmospheric boundary layer.

608 The obtained results are undoubtedly of interest for the further development of the aero-
609 dynamics of wind turbines and wind farms, both to optimize the operation of existing FW, and
610 to design and analyze the new ones. The findings formulated above in the description of the
611 studied phenomena will be useful to improve the energy and economic efficiency, reliability
612 and safety of impellers of axial turbines in wind power. In addition, the conducted research
613 gives an impetus to new works related to further development of the FW. New research is nec-
614 essary to complete the study on the selection of optimal shapes for the wind turbine blades.
615 The question on the influence of the difference in the axial shape of the blades on the gas tur-
616 bine performance should be answered in order to assess the theoretical solutions, predicting
617 greater efficiency of the blades with constant distribution of circulation compared with
618 the Goldstein circulation.

619 Important is the question about the influence of turbulent fluctuations of the incident flow
620 on the efficiency of wind turbines. It is necessary to investigate the model setups at elevated
621 levels of free-stream turbulence and compare them with the available data for almost turbu-
622 lence-free mode. The study of the impact of various obstacles on the operation of wind turbines
623 should be continued as well.

624 The last important point of new research is reconsideration and correct modeling of
625 the effect of stabilizing of the generated power in the chain of wind turbines located in the wakes
626 one behind another. Here, attention should be paid to the impact of perturbations in the wakes
627 of previous turbines on the development of the near wake of subsequent turbines and to the use
628 of additional generation of various disturbances with the view of revealing the dynamics of
629 the near wake destruction.

630 The above stated questions for new studies will undoubtedly give an impetus to new
631 development of aerodynamics of wind turbines and wind farms.

632 The author is grateful to I.V. Naumov and V.I. Litvinov for helpful comments during
633 the preparation of the manuscript.

634

References

- 635 S.V. Alekseenko, P.A. Kuibin, and V.L. Okulov, 2007, Theory of Concentrated Vortices: an Introduction, Springer-
636 Verlag, Berlin-Heidelberg.
- 637 P. Bachant and M. Wosnik, 2015, Characterising the near-wake of a cross-flow turbine, *J. Turbulence*, Vol. 16,
638 No. 4, P. 392–410.
- 639 R.J. Barthelmie, K. Hansen, S.T. Frandsen, O. Rathmann, J.G. Schepers, W. Schlez, J. Phillips, K. Rados,
640 A. Zervos, E.S. Politis, and P.K. Chaviaropoulos, 2009, Modeling and measuring flow and wind turbine wakes
641 in large wind farms offshore, *Wind Energy*, Vol. 12, No. 5, P. 431–444.
- 642 J. Bartl, F. Pierella, and L. Sætran, 2012, Wake measurements behind an array of two model wind turbines, *Energy*
643 *Procedia*, Vol. 24, P. 305–312.
- 644 M. Bastankhan and F. Porté-Agel, 2014, A new analytical model for wind turbine wakes, *Renewable Energy*,
645 Vol. 70, P. 116–123.

- 646 **M. Bastankhan and F. Porté-Agel**, 2016, Experimental and theoretical study of wind turbine wakes in yawed
647 conditions, *J. Fluid Mech.*, Vol. 806, P. 506–541.
- 648 **A. Betz**, 1919, Schraubenpropeller mit geringstem Energieverlust: mit einem Zusatz von L. Prandtl, Göttinger
649 Nachrichten 196, bis 217, Göttingen.
- 650 **L.P. Chamorro, C. Hill, S. Morton, C. Ellis, R.E.A. Arndt, and F. Sotiropoulos**, 2013, On the interaction between
651 a turbulent open channel flow and an axial-flow turbine, *J. Fluid Mech.*, Vol. 716, P. 658–670.
- 652 **G.V. Ermolenko, I.G. Gordeev, A.V. Nikomarova, M.A. Ryzhnikov, and V.N. Tskhomariya**, 2012, Pilot projects
653 of network wind power in the Eisk region of Krasnodar krai: The state and prospects, *Therm. Engng*, Vol. 59,
654 No. 11, P. 846–853.
- 655 **N.P. Dufresne and M. Wosnik**, 2013, Velocity deficit and swirl in the turbulent wake of a wind turbine, *J. Marine
656 Technology Society*, Vol. 47, No. 4, P. 193–205.
- 657 **M. Felli, R. Camussi, and F. Di Felice**, 2011, Mechanisms of evolution of the propeller wake in the transition and far
658 fields, *J. Fluid Mech.*, Vol. 682, P. 5–53.
- 659 **O.A.H. Flamm**, Die Schiffschraube und ihre Wirkung auf das Wasser, Berlin, 1909.
- 660 **V.E. Fortov and O.S. Popel'**, 2014, The current status of the development of renewable energy sources worldwide
661 and in Russia, *Therm. Engng*, Vol. 61, No. 6, P. 389–398.
- 662 **P. Fraunie, C. Beguier, I. Paraschivoiu, and G. Brochier**, Water channel experiments of dynamic stall on Darrieus
663 wind turbine blades, *J. Propulsion and Power*, 1986, Vol. 2, No. 5, P. 445–449.
- 664 **R.E. Froude**, 1889, On the part played in propulsion by differences of fluid pressure, *Trans. Inst. Naval Architects*,
665 Vol. 30, P. 390–405.
- 666 **R.E. Froude**, 1911, The acceleration in front of a propeller, *Trans. Inst. of Naval Architects*, Vol. 53, P. 139–182.
- 667 **Y. Fukumoto, V.L. Okulov, and D.H. Wood**, 2015, The contribution of Kawada to the analytical solution for
668 the velocity induced by a helical vortex filament, *ASME Appl. Mech. Rev.*, Vol. 67, No. 6, P. 060801.
- 669 **W.K. George**, 1989, The self-preservation of turbulent flows and its relation to initial conditions and coherent structures,
670 *Advances in Turbulence*, W.K. George and R. Anndt. (Eds.), Hemisphere Publ. Corp., N.Y., P. 39–73.
- 671 **H. Glauert**, 1935, Airplane propellers: Division L, Aerodynamic Theory IV, W.F. Durand (Ed.), P. 169–360, Springer,
672 Berlin.
- 673 **S. Goldstein**, 1929, On the vortex theory of screw propellers, *Proc. Roy. Soc. London A*, Vol. 123, P. 440–465.
- 674 **A.K. Gupta**, 2015, Efficient wind energy conversion: evolution to modern design, *J. Energy Resour. Technol.*,
675 Vol. 137, No. 5, P. 051201-1–051201-10.
- 676 **N. Jensen**, 1983, A note on wind turbine interaction, Technical report Ris-M-2411, Roskilde, Denmark: Risø National
677 Laboratory.
- 678 **F. Jiang, H.I. Andersson, J.P. Gallardo, and V.L. Okulov**, 2016, On the peculiar structure of a helical wake vortex
679 behind an inclined prolate spheroid, *J. Fluid Mech.*, Vol. 801, P. 1–12.
- 680 **P.B. Johansson, and W.K. George**, The far downstream evolution of the high-Reynolds number axisymmetric wake
681 behind a disk. Part 1. Single-point statistics, *J. Fluid Mech.*, 2006, Vol. 555, P. 363–385.
- 682 **N.E. Joukowski**, 1912, Vortex theory of screw propeller I, *Trudy Otdeleniya Fizicheskikh Nauk Obshchestva
683 Lubitelei Estestvoznaniya*, Vol. 16, Iss. 14, P. 1–31.
- 684 **N.E. Joukowski**, 1914, Vortex theory of screw propeller II, *Trudy Otdeleniya Fizicheskikh Nauk Obshchestva
685 Lubitelei Estestvoznaniya*, Vol. 17, Iss. 1.
- 686 **N.E. Joukowski**, 1915, Vortex theory of screw propeller III, *Trudy Otdeleniya Fizicheskikh Nauk Obshchestva
687 Lubitelei Estestvoznaniya*, Vol. 18, Iss. 2.
- 688 **N.E. Joukowski**, 1918, Vortex theory of screw propeller IV, *Trudy Avia Raschetno-Ispytatel'nogo Byuro*, Vol. 3–4,
689 P. 1–97.
- 690 **M.O.L. Hansen**, 2008, Aerodynamics of Wind Turbines, Earthscan (Ed.).
- 691 **M. Hand, D. Simms, L. Fingersh, D. Jager, J. Cotrell, S. Schreck, and S. Larwood**, 2001, Unsteady aerodynamics
692 experiment phase vi: Wind tunnel test configurations and available data campaigns, Technical report NREL/TP.
693 No. 500-29955.
- 694 **Th. van Holten**, 1981, Concentrator systems for wind energy, with emphasis on tip-vanes, *Wind Engng*, Vol. 5, No. 1,
695 P. 29–45.
- 696 **J. Hong, M. Toloui, L.P. Chamorro, and M. Guala**, 2014, Natural snowfall reveals large-scale flow structures
697 in the wake of a 2.5-MW wind turbine, *Nature Communications*, Vol. 5, No. 4216, P. 1–9.
- 698 **G.A.M. van Kuik**, Momentum theory of Joukowski actuator discs with swirl, *J. Physics: Conference Series*, IOP
699 Publishing, 2016, Vol. 753, No. 2, P. 022021.
- 700 **G.A.M. van Kuik, J.N. Sørensen, and V.L. Okulov**, 2015, Rotor theories by professor Joukowski: Momentum theories,
701 *Progress in Aerospace Sciences*, Vol. 73, P. 1–18.
- 702 **G.C. Larsen, H.A. Madsen, F. Bingöl, J. Mann, S. Ott et al.**, 2007, Dynamic wake meandering modeling, Risø
703 National Laboratory.
- 704 **T. J. Larsen, H.A. Madsen, G.C. Larsen, and K.S. Hansen**, 2013, Validation of the dynamic wake meander model
705 for loads and power production in the Egmond aan Zee wind farm, *Wind Energy*, Vol. 16, No. 4, P. 605–624.
- 706 **I.V. Litvinov, I.V. Naumov, V.L. Okulov, and R.F. Mikkelsen**, 2015, Comparison of far wake behind solid disk and
707 three blades rotor, *J. Flow Visualization and Image Processing*, Vol. 22, No. 4, P. 175–183.

- 708 **D. Medici and P.H. Alfredsson**, 2006, Measurements on a wind turbine wake: 3D effects and bluff body vortex
709 shedding, *Wind Energy*, Vol. 9, P. 219–236.
- 710 **I.V. Naumov, I.K. Kabardin, R.F. Mikkelsen, V.L. Okulov, and J.N. Sørensen**, Performance and wake conditions
711 of a rotor located in the wake of an obstacle, *J. Phys.: Conference Series*. IOP Publishing, 2016, Vol. 753, No. 3,
712 P. 032051.
- 713 **I.V. Naumov, I.K. Kabardin, R.F. Mikkelsen, V.L. Okulov, and J.N. Sørensen**, 2017, An influence of the different
714 incoming wake-like flows on the rotor vibrations, *J. Phys.: Conference Series*. IOP Publishing, Vol. 854,
715 P. 012034.
- 716 **I.V. Naumov, I.V. Litvinov, R.F. Mikkelsen, and V.L. Okulov**, 2015, Investigation of a wake decay behind a circu-
717 lar disk in a hydro channel at high Reynolds numbers, *Thermophysics and Aeromechanics*, Vol. 22, No.6,
718 P. 657–665.
- 719 **I.V. Naumov, I.V. Litvinov, R.F. Mikkelsen, and V.L. Okulov**, 2016, Experimental investigation of wake evolution
720 behind a couple of flat discs in a hydrochannel, *Thermophysics and Aeromechanics*, Vol. 23, No. 5, P. 657–666.
- 721 **I.V. Naumov, R.F. Mikkelsen, and V.L. Okulov**, 2016, Estimation of wake propagation behind the rotors of wind-
722 powered generators, *Thermal Engineering*, Vol. 63, No. 3, P. 208–213.
- 723 **I.V. Naumov, R.F. Mikkelsen, V.L. Okulov, and J.N. Sørensen**, 2014, PIV and LDA measurements of the wake
724 behind a wind turbine model, *J. Phys.: Conference Series*, Vol. 524, P. 012168.
- 725 **I.V. Naumov, V.V. Rakhmanov, V.L. Okulov, K.M. Velta, K.E. Mayer, and R.F. Mikkelsen**, 2012, Flow diagnostics
726 downstream of a tribladed rotor model, *Thermophysics and Aeromechanics*, Vol. 19, No. 2, P. 268–278.
- 727 **V.S. Neary, B. Gunawan, C. Hill, and L.P. Chamorro**, 2013, Near and far field flow disturbances induced by model
728 hydrokinetic turbine: ADV and ADP comparison, *Renewable Energy*, Vol. 60, P. 1–6.
- 729 **B.G. Novikov**, 2009, Effect of small total pulse on development of a wake behind the self-propelled bodies,
730 *Thermophysics and Aeromechanics*, Vol. 16, No. 4, P. 561–583.
- 731 **N.G. Nygaard**, Wakes in very large wind farms and the effect of neighbouring wind farms, *J. Phys.: Conference*
732 *Series*. IOP Publishing, 2014, Vol. 524, No. 1, P. 012162.
- 733 **V.L. Okulov**, Limit cases for rotor theories with Betz optimization, *J. Phys.: Conference Series*. IOP Publishing, 2014,
734 Vol. 524, No. 1, P. 012129.
- 735 **V.L. Okulov**, 2016, An acentric rotation of two helical vortices of the same circulations, *Regular and Chaotic*
736 *Dynamics*, Vol. 21, No. 3, P. 267–273.
- 737 **V.L. Okulov, I.V. Litvinov, R.F. Mikkelsen, I.V. Naumov, and J.N. Sørensen**, 2017a, Wake developments behind
738 different configurations of passive disks and active rotors, *J. Phys.: Conference Series*. IOP Publishing, Vol. 854,
739 P. 012035.
- 740 **V.L. Okulov, I.V. Litvinov, I.V. Naumov, and R. Mikkelsen**, 2017b, Self-similarity of far wake behind tandem of
741 two disks, *J. Engng Thermophysics*, Vol. 26, No. 2, P. 154–159.
- 742 **V.L. Okulov, R.F. Mikkelsen, I.V. Litvinov, and I.V. Naumov**, Efficiency of operation of wind generator rotors
743 optimized by the Glauert and Betz methods, *Techn. Phys.*, 2015, Vol. 60, No. 11, P. 1632–1636.
- 744 **V.L. Okulov, R.F. Mikkelsen, I.V. Naumov, I.V. Litvinov, E. Gesheva, and J.N. Sørensen**, 2016, Comparison of
745 the far wake behind dual rotor and dual disk configurations, *J. Phys.: Conference Series*. IOP Publishing, Vol. 753,
746 No. 3, P. 032060.
- 747 **V.L. Okulov, R.F. Mikkelsen, J.N. Sørensen, I.V. Naumov, and M.A. Tsoy**, 2017, Power properties of two interact-
748 ing wind turbine rotors, *ASME. J. Energy Resour. Technol.*, Vol. 139, No. 5, P. 051210-1–051210-6.
- 749 **V.L. Okulov, I.V. Naumov, R.F. Mikkelsen, I.K. Kabardin, and J.N. Sørensen**, 2014, A regular Strouhal number
750 for large-scale instability in the far wake of a rotor, *J. Fluid Mech.*, Vol. 747, P. 369–380.
- 751 **V.L. Okulov, I.V. Naumov, R.F. Mikkelsen, and J.N. Sørensen**, 2015, Wake effect on a uniform flow behind wind-
752 turbine model, *J. Phys.: Conference Series*. IOP Publishing, Vol. 625, No. 1, P. 012011.
- 753 **V.L. Okulov, I.V. Naumov, and J.N. Sørensen**, 2007, Optical diagnostics of intermittent flows, *Techn. Phys.*, Vol. 77,
754 No. 5, P. 47–57.
- 755 **V.L. Okulov, I.V. Naumov, M.A. Tsoi, and R.F. Mikkelsen**, 2017, Loss of efficiency in coaxial arrangement of
756 the pair of wind turbines, *Thermophysics and Aeromechanics*, Vol. 24, No. 4, P. 545–551.
- 757 **V.L. Okulov and J.N. Sørensen**, 2007, Stability of helical tip vortices in a rotor far wake, *J. Fluid Mech.*, Vol. 576,
758 P. 1–25.
- 759 **V.L. Okulov and J.N. Sørensen**, 2008, Refined betz limit for rotors with a finite number of blades, *Wind Energy*,
760 Vol. 11, No. 4, P. 415–426.
- 761 **V.L. Okulov and J.N. Sørensen**, 2010a, Applications of 2D helical vortex dynamics, *Theor. Comput. Fluid Dyn.*,
762 Vol. 24, P. 395–401.
- 763 **V.L. Okulov and J.N. Sørensen**, 2010b, Maximum efficiency of wind turbine rotors using Joukowsky and Betz ap-
764 proaches, *J. Fluid Mech.*, Vol. 649, P. 497–508.
- 765 **V.L. Okulov, J.N. Sørensen, and W.Z. Shen**, 2016, Expansion of Goldstein's circulation function for optimal rotors
766 with hub, *J. Phys.: Conference Series*. IOP Publishing, Vol. 753, No. 2, P. 022018.
- 767 **V.L. Okulov, J.N. Sørensen, and G.A.M. van Kuik**, 2013, Development of the Optimum Rotor Theories, Moscow-
768 Izhevsk: R&C Dyn.
- 769 **V.L. Okulov, J.N. Sørensen, and D.H. Wood**, 2015, The rotor theories by professor Joukowsky: Vortex theories,
770 *Progress in Aerospace Sci.*, Vol. 73, P. 19–46.

- 771 **H.U. Quaranta and T. Leweke**, 2015, Long-wave instability of a helical vortex, *J. Fluid Mech.*, Vol. 780,
772 P. 687–716.
- 773 **W.J.M. Rankine**, 1865, On the mechanical principles of the action of propellers, *Trans. Inst. Naval Architects*, Vol. 6,
774 P. 13–39.
- 775 **A.Segalini and P. Inghels**, 2014, Confinement effects in wind-turbine and propeller measurements, *J. Fluid Mech.*,
776 Vol. 756, P. 110–129.
- 777 **M.S. Selig, J.J. Guglielmo, A.P. Broeren, and P. Giguere**, 1995, Summary of Low-Speed Airfoil Data, Vol. 1,
778 SolarTech Publication.
- 779 **J.N. Sørensen**, 2016, General Momentum Theory for Horizontal Axis Wind Turbines, Springer.
- 780 **J.N. Sørensen and G.A.M. van Kuik**, 2010, General momentum theory for wind turbines at low tip speed ratios,
781 *Wind Energy*, Vol. 14, P. 821–839.
- 782 **J.N. Sørensen, R.F. Mikkelsen, N. Troldborg, V. Okulov, and W.Z. Shen**, 2013, The aerodynamics of wind
783 turbines, in: *Proc. 22nd Int. Congress of Theoretical and Applied Mechanics, ICTAM 2008*, P. 231–247,
784 Mechanics Down Under.
- 785 **J.N. Sørensen, V.L. Okulov, R.F. Mikkelsen, I.V. Naumov, and I.V. Litvinov**, 2016, Comparison of classical
786 methods for blade design and the influence of tip correction on rotor performance, *J. Phys.: Conference Series*. IOP
787 Publishing, Vol. 753, No. 2, P. 022020.
- 788 **B.M. Sumer and J. Fredøse**, 2006, Hydrodynamics around cylindrical structures, *Advanced Series on Ocean Engi-*
789 *neering* 26, World Scientific.
- 790 **B. Sunden and Z. Wu**, 2015, On icing and icing mitigation of wind turbine blades in cold climate, *J. Energy Resour.*
791 *Technol.*, Vol. 137, No. 5, P. 051203-1–051203-10.
- 792 **K.W. van Treuren**, 2015, Small-scale wind turbine testing in wind tunnels under low Reynolds number conditions,
793 *J. Energy Resour. Technol.*, Vol. 137, No. 5, P. 051208-1–051208-11.
- 794 **L. Vermeer, J.N. Sørensen, and A. Crespo**, 2003, Wind turbine wake aerodynamics, *Progress in Aerospace Sci.*,
795 Vol. 39, P. 467–510.
- 796 **O.F. Voropaeva, O.A. Druzhinin, and G.G. Chernykh**, 2016, Numerical simulation of momentumless turbulent
797 wake dynamics in linearly stratified medium, *J. Engng Thermophysics*, Vol. 25, No. 1, P. 85–99.
- 798 **Q.R. Wald**, 2006, The aerodynamics of propellers, *Progress in Aerospace Sci.*, Vol. 42, No. 2, P. 85–128.
- 799 **J.H. Walther, M. Guenot, E. Machefaux, J.T. Rasmucsen et al.**, 2007, A numerical study of the stability of helical
800 vortices using vortex methods, *J. Phys.: Conference Series*. IOP Publishing, Vol. 75, No. 1, P. 012034.
- 801 **D.H. Wood and V.L. Okulov**, 2017, Nonlinear blade element-momentum analysis of Betz-Goldstein rotors, *Renewable*
802 *Energy*, Vol. 107, P. 542–549.
- 803 **D.H. Wood, V.L. Okulov, and D. Bhattacharjee**, 2016, Direct calculation of wind turbine tip loss, *Renewable Ener-*
804 *gy*, Vol. 95, P. 269–276.
- 805 **J. Yang, M. Liu, G. Wu, W. Zhong, and X. Zhang**, 2014, Numerical study on coherent structure behind a circular
806 disk, *J. Fluids Struct.*, Vol. 51, P. 172–188.